Available online at www.sciencedirect.com
SCIENCE DIRECT®
Carbohydrate Polymers xxx (2006) xxx–xxx
Carbohydrate Polymers
www.elsevier.com/locate/carbpol

Properties of biocomposites based on lignocellulosic fillers

L. Avérous [a,*], F. Le Digabel [b]

[a] LIPHT, ECPM, Université Louis Pasteur, 25 rue Becquerel, 67087 Strasbourg Cedex 2, France
[b] UMR FARE INRA/URCA, BP 1039, 51687 Reims Cedex 2, France

Received 15 December 2005; received in revised form 15 March 2006; accepted 1 April 2006

Abstract

This paper is focused on the analysis of the thermal and mechanical behaviour of processed biocomposites (biodegradable composites). These materials have been created by extrusion and injection moulding. The matrix, a biodegradable and aromatic copolyester (polybutylene adipate-co-terephthalate), has been fully characterised (NMR, SEC). The lignocellulosic materials used as fillers are a by-product of an industrial fractionation process of wheat straw. Different filler fractions have been selected by successive sieving, and then carefully analysed (granulometry, chemical structure). Cellulose, lignin, and hemicellulose contents have been determined through different techniques. The biocomposites thermal behaviour has been investigated by TGA (thermal degradation) and DSC (transition temperatures, crystallinity). These materials present good mechanical behaviour due to high filler-matrix compatibility. The impacts of filler content, filler size and the nature of each fraction have been analysed. To predict the mechanical behaviour, Takayanagi's equation seems to provide an accurate answer to evaluate the modulus in a range, 0–30 wt% of fillers.

Keywords: Biocomposite; Biodegradable; Lignocellulosic fillers; Mechanical properties

1. Introduction

Tailoring new composites within a perspective of sustainable development or eco-design, is a philosophy that is applied to more and more materials. Ecological concerns have resulted in a renewed interest in natural, renewable resources-based and compostable materials, and therefore issues such as materials elimination and environmental safety are becoming important. For these reasons, material components such as natural fibres, biodegradable polymers can be considered as "interesting" – environmentally safe – alternatives for the development of new biodegradable composites (biocomposites).

The classification of biodegradable polymers in different families has been published and presented elsewhere (Avérous, 2004). Agro-polymers (e.g., polysaccharides) are the first family. They are obtained from biomass by fractionation. The polyesters obtained by fermentation from biomass or from genetically modified plants (e.g., polyhydroxyalkanoate: PHA) are the second group. Polymers of the third family are synthesised from monomers obtained from biomass (e.g., polylactic acid: PLA). Fourth and last family are polyesters totally synthesised by petrochemical process (e.g., polycaprolactone: PCL, polyesteramide: PEA, aliphatic or aromatic copolyesters), from fossil resources. A large number of these biodegradable polymers are commercially available. They show a large range of properties and at present, they can compete with non-biodegradable polymers in different industrial fields (e.g., packaging, agriculture, hygiene, and cutlery).

Lignocellulose-based fibres are the most widely used, as biodegradable filler. Intrinsically, these fibres have a number of interesting mechanical and physical properties (Bledzki & Gassan, 1999; Mohanty, Misra, & Hinrichsen, 2000; Saheb & Jog, 1999). These renewable materials present strong variations according to the botanical origin (Table 1). With their environmentally friendly character and some techno-economical advantages, these fibres

* Corresponding author. Tel.: +33 03 90 24 27 07; fax: +33 03 90 24 27 16.
E-mail address: AverousL@ecpm.u-strasbg.fr (L. Avérous).

0144-8617/$ - see front matter © 2006 Elsevier Ltd. All rights reserved.
doi:10.1016/j.carbpol.2006.04.004

Table 1
Chemical composition (wt%) of vegetable fibers

Fiber	Cellulose	Hemicellulose	Pectin	Lignin	Ash
Bast fibers					
Flax[a]	71	19	2	2	1–2
Hemp[a]	75	18	1	4	1–2
Jute[a]	72	13	>1	13	8
Ramie[a]	76	15	2	1	5
Leaf fibers					
Abaca[a]	70	22	1	6	1
Sisal[a]	73	13	1	11	7
Seed-hair fibers					
Cotton[a]	93	3	3	–	1
Wheat straw[a]	51	26	–	16	7
LCF fillers					
$LCF_{0–1}$	58	8	–	31	3
$LCF_{0–0.1}$	56	7	–	31	6
$LCF_{0.1–1}$	59	8	–	31	2

[a] *Sources*: Young, 2004; Le Digabel, 2004.

motivate more and more different industrial sectors (automotive) to replace common fibreglass, for example.

Biocomposites are obtained by the combination of biodegradable polymer as the matrix material and biodegradable fillers (e.g., lignocellulosic fillers). Since both components are biodegradable, the composite as the integral part is also expected to be biodegradable (Mohanty et al., 2000). For short-term applications, biocomposites present strong advantages, and a large number of papers has been published on this topic. Except some publications based on polysaccharide matrix (e.g., plasticized starch) (Avérous & Boquillon, 2004; Avérous, Fringant, & Moro, 2001) most of the published studies (Avérous, 2004) are based on biopolyesters (biodegradable polyesters) matrices (Mohanty et al., 2000; Netravali & Chabba, 2003). For instance, PHA has been combined with lignocellulosic fibres (Bourban et al., 1997; Wollerdorfer & Bader, 1998), jute fibres (Mohanty, Khan, & Hinrichsen, 2000a; Wollerdorfer & Bader, 1998), abaca fibres (Shibata, Takachiyo, Ozawa, Yosomiya, & Takeishi, 2002), pineapple fibres (Luo & Netravali, 1999), flax fibres (Van de Velde & Kiekens, 2002), wheat straw fibres (Avella et al., 2000) or lignocellulosic flour (Dufresne, Dupeyre, & Paillet, 2003; Fernandes, Pietrini, & Chiellini, 2004). PLA has been associated with paper waste fibres, wood flour (Levit, Farrel, Gross, & McCarthy, 1996), kenaf (Nishino, Hirao, Kotera, Nakamae, & Inagaki, 2003), jute (Plackett, Logstrup Andersen, Batsberg Pedersen, & Nielsen, 2003) or flax fibres (Oksman, Skrifvars, & Selin, 2003; Van de Velde & Kiekens, 2002). Some authors have tested flax (Van de Velde & Kiekens, 2002) or sisal (Ruseckaite & Jiménez, 2003) with PCL. Mohanty, Khan, and Hinrichsen (2000b) have reinforced PEA with jute fibres. Aliphatic copolyesters have been used with cellulosic fibres (Wollerdorfer & Bader, 1998), bamboo fibres (Kitagawa, Watanabe, Mizoguchi, & Hamada, 2002) or flax, oil palm, jute or ramie fibres (Wollerdorfer & Bader, 1998). Aromatic copolyesters have been associated with wheat straw fillers. Some results on such systems are presented in a previous publication (Le Digabel, Boquillon, Dole, Monties, & Avérous, 2004). Le Digabel et al. (2004) have shown a good compatibility between the fillers and the biodegradable matrix without compatibilizers or special fillers treatment.

This paper is focussed on the processing and on the analysis of biocomposites based on lignocellulosic fillers (LCF) which are by-products of an industrial fractionation of wheat straw. These fillers are combined with biodegradable aromatic copolyester, polybutylene adipate-co-terephthalate (PBAT). The use of low cost bio-fillers is a way to reduce the cost of the end product with improved properties. The aim of this paper is more particularly targeted at the thermal and mechanical properties of these biocomposites. We have analysed the influence of the filler size and content and, we have tried to predict by modelling the corresponding evolution of the modulus. This paper complements and expands a previous publication (Le Digabel et al., 2004).

2. Experimental

2.1. Materials

The matrix, a biodegradable and aromatic copolyester (polybutylene adipate-co-terephthalate, PBAT) has been kindly supplied by Eastman (EASTAR BIO Ultra Copolyester 14766). Copolyester chemical structure is drawn in Fig. 1. This copolyester is soluble at room temperature in different solvents such as THF, CH_2Cl_2 and $CHCl_3$. The ratio between each monomer has been determined by ^1H NMR. Fig. 2 shows the NMR spectrum of PBAT, dissolved in chloroform. The integration of the adequate peaks (2.33 and 8.1 ppm) gives PBAT composition, 43% of butylene terephthalate and 57% of butylene adipate. Molecular weight (M_w) and polydispersity index (IP) are 48,000 and 2.4, respectively. They have been determined by size exclusion chromatography (SEC). Melt flow index (MFI) is 13 g/10 mn at 190 °C/2.16 kg. PBAT density is 1.27 g/cm^3 at 23 °C.

The lignocellulosic materials used as fillers are a by-product of an industrial fractionation process of wheat straw (ARD, Pomacle, France). This product is obtained

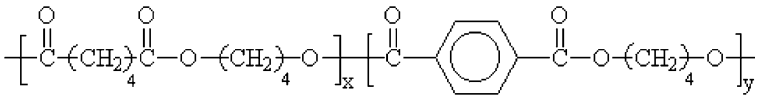

Fig. 1. Chemical structure of the copolyester (PBAT).

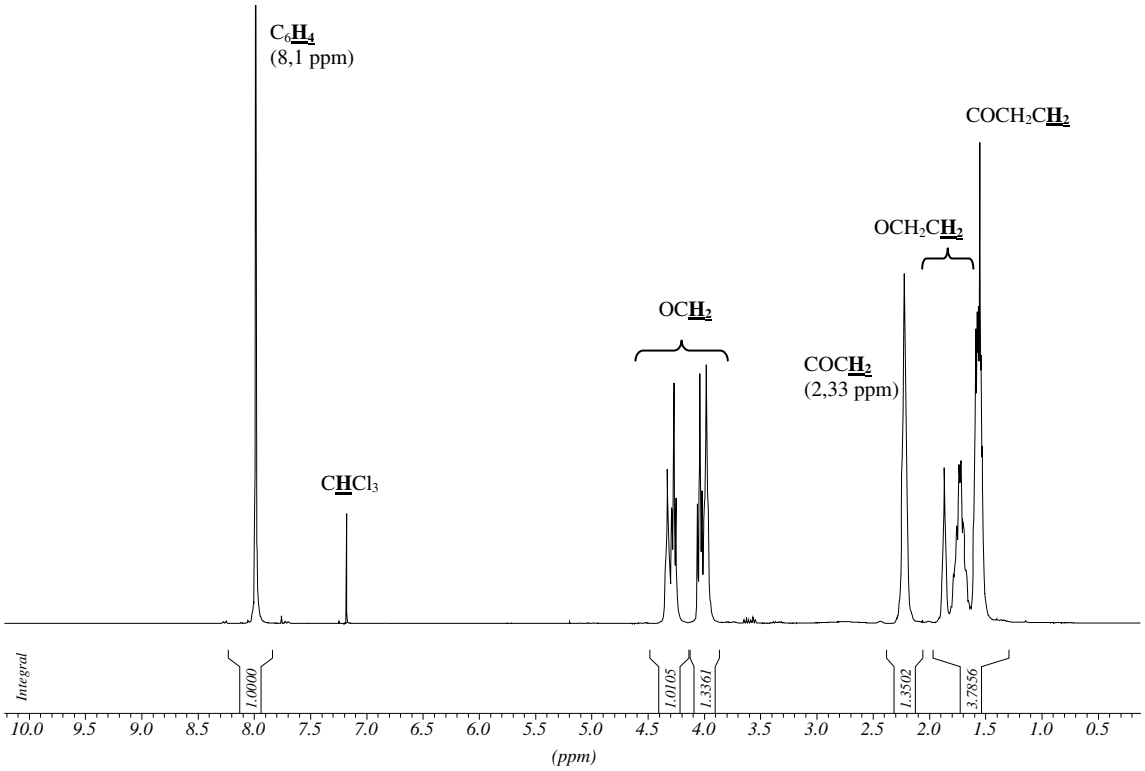

Fig. 2. ^{1}H NMR spectrum of PBAT.

from a multi-step process. 250 kg of chopped wheat straw (10–15 cm) are introduced into a 1 m^3 reactor under high shearing to promote fibre fragmentation. Wheat straw is hydrolysed in acid medium (H_2SO_4, 0.1 N) under pressure (3.5 bars) at 130 °C, during maintenance of 90 mn (Roller, 1990). The soluble fraction (mostly hemicellulose sugars) is filtered and refined for further applications. The insoluble fraction, the by-product called lignocellulosic filler (LCF) is neutralised, washed and dried with a turbo-dryer (Alpha Vomm, Italy). The process yield from the wheat straw to the LCF is 33%. The dried LCF filler is sieved with a 1 mm grid to eliminate the biggest fillers (20 wt%). This product is named LCF_{0-1}. According to Fig. 3, this last fraction is sieved with a 0.1 mm grille and then two fractions are obtained, $LCF_{0.1-1}$ and $LCF_{0-0.1}$.

2.2. Biocomposites processing

In a previous publication, we have shown that the filler-matrix interactions are sufficient to avoid filler treatment and/or addition of compatibilizers, which are costly. Prior to blending, fillers and thermoplastic granules are dried in an air-circulating oven at 80 °C, for up to 4 and 1 h, respectively. PBAT and varying amounts of LCF are directly added in the feeding zone of a single screw extruder (SCAMIA S 2032, France) equipped with a specific designed torpedo-like element to promote high shearing and mixing. The screw diameter (D) and the L/D ratio are 30 mm and 26/1, respectively. Typically, for technical reasons due to the quality of the filler dispersion, the maximum LCF content is 30–40 wt%. Extrusion temperature is 135 °C. Three millimetre diameter strands are pelletized after air-cooling. These granules are extruded once again at the same condition to improve the filler dispersion into the matrix.

Standard dumbbell test pieces (NFT 51-034-1981) are moulded with an injection moulding machine (DK codim NGH 50/100) in a temperature range between 115 and 130 °C, with an injection pressure and speed of 500 bars and 50 mm/s. Holding pressure and times are 500 bars and 12 s (PBAT) or 14 s (biocomposites), respectively. Mould temperature is 30 °C. The total cooling time is 22 s (neat PBAT) and 24 s. The injection-moulded specimens are approximately 10 mm wide and 4 mm thick in the central part (French standard NFT 51-0.34 1981).

2.3. Characterisations

PBAT molecular weights and polydispersity index have been determined by SEC with PS standards for the calibration. Analyses are performed in THF on two PL-gel 5 μm mixed-C, a 5 μm 100 Å and a 5 μm Guard columns in a Shimadzu LC-10AD liquid chromatograph equipped with a Shimadzu RID-10A refractive index detector and a Shimadzu SPP-M10A diode array UV detector.

NMR equipment is a NMR 300 MHz (Bruker 300 Ultrashield, USA). Samples have been dissolved in deuterated chloroform.

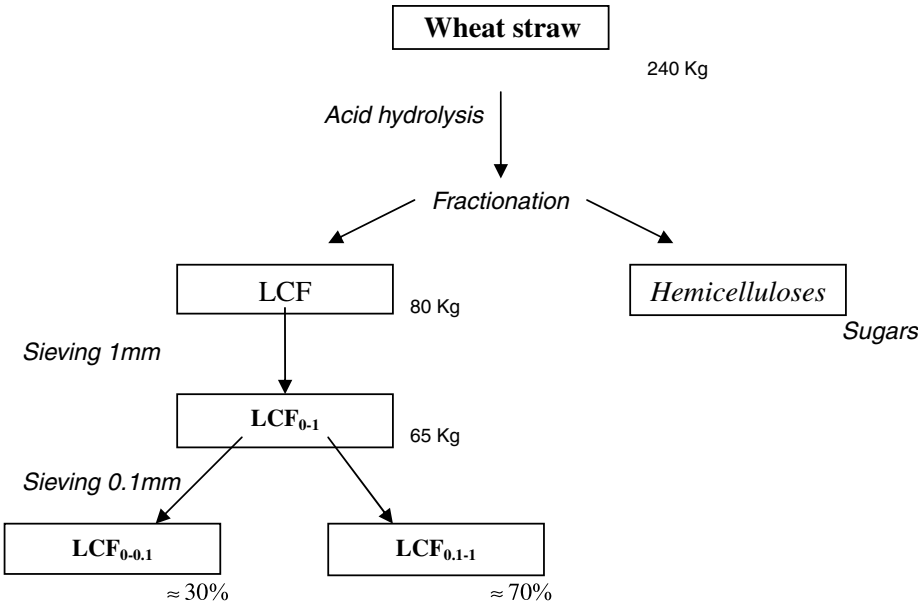

Fig. 3. Fillers fractions elaboration: wheat straw fractioning schema.

The fillers size distributions have been determined by light scattering with a particles size analyzer (Mastersizer 2000, Malvern Instruments, UK), in a 10 nm–2 mm range.

Optical observations of the fillers are performed with a transmission/reflection microscope (Zeiss, Germany). Scanning electron microscopy (SEM) is performed with a LEO Gemini 98 (USA) instrument to investigate the filler morphology, at low voltage without metal coating.

The composition of the fillers is determined. Lignin and mineral contents are determined by Klason lignin method, according to the protocol described by Monties (1984). For each sample, 300 mg (M) are added to 3 ml H_2SO_4. After 2 h at 20 °C, the solution is diluted into 40 ml of distilled water. Then, the mix is carried out at reflux for 3 h. After filtration, the solid residue is washed several times with distilled water until neutrality of the filtrate is obtained. The residue is dried at 100 °C for 20 h and weighted (P_1). This residue is calcinated at 500 °C for 210 min and then weighted (P_2) to determine the mineral content. Three samples are analysed for each filler fraction. The Klason lignin content is determined according to Eq. (1).

$$\text{Lignins(KL)} = \frac{P_1 - P_2}{M} \quad (1)$$

After acid hydrolysis (H_2SO_4) and filtration to eliminate lignin and minerals, sugar titration allowed quantifying the cellulose and hemicellulose contents according to the procedure described by Lequart, Ruel, Lapierre, Pollet, and Kurek (2000). This analysis is carried out with high performance liquid chromatography (HPLC) with a Dionex© column (anion exchange column). During the analysis, the different dissolved sugars are ionized with NaOH (0.1 N) which is the mobile phase. The glucose concentration gives the cellulose content. The different sugars obtained from hemicellulose hydrolysis are also quantified.

The filler density is determined by pycnometry measurements on 10, 20, and 30% LCF filled biocomposites (injected samples) assuming there are no voids in the tested biocomposites.

The thermal stability is determined by thermo-gravimetric analysis with a high resolution TGA (2950 WATERS TA Instruments, USA) at a heating rate of 20 °C min^{-1} from 30 to 550 °C. Degradation temperatures are determined on DTG scans, at the peak maximum.

Differential scanning calorimeter (DSC 2920, TA Instruments, USA) is used. Samples (between 10 and 15 mg) are sealed in aluminium pans. The heating and cooling rates are 10 °C min^{-1}. A nitrogen flow (45 ml min^{-1}) is maintained throughout the test. For all materials, the first scan is used for eliminating the thermal history of the material. Each sample is heated to 150 °C then cooled to −50 °C before a second heating scan to 150 °C. The glass transition temperature (T_g) and melting temperature (T_m) are determined from the second heating scan. The crystallisation temperature (T_c) is obtained from the cooling scan because the samples are not quenched. The temperature of induction (T_i) is the beginning of the crystallization during the cooling. T_g is determined at the mid-point of heat capacity changes, T_m at the onset peak of the endothermic and T_c at the onset peak of the exothermic. Three samples for each blend are tested. By integration of the corresponding peaks, we have determined the different heats of crystallization and fusion (ΔH_c and ΔH_f). These values (determined in J/g) can be corrected from a dilution effect linked to the fillers incorporation into the matrix e.g., see Eq. (2) where ww is the filler fraction.

$$\Delta H_c' = \frac{\Delta H_c}{1 - ww} \quad (2)$$

The degree of crystallinity (in %) can be estimated with Eq. (3).

$$X_c(\%) = \frac{\Delta H_f}{\Delta H_{100\%}} \times \frac{100}{1 - ww} \quad (3)$$

Tensile testing is carried out with an Instron Universal Testing Machine (model 4204) in tensile mode, according to the ASTM D882-91, with a crosshead speed of 50 mm min^{-1}. Ten samples for each formulation are tested. Before testing to stabilize the different specimens, storage conditions are 23 °C and 50% RH (Relative Humidity) for 5 days. The non-linear mechanical behaviour of the different samples is determined through different parameters. The nominal and the true strains are given by Eqs. (4) and (5), respectively. In these equations, L and L_0 are the length during the test and at zero time, respectively. Two different strains are calculated; strain at the yield point (ε_Y) and at break (ε_b).

$$\langle \varepsilon \rangle = \frac{L - L_0}{L_0} \quad (4)$$

$$\varepsilon = Ln\left(\frac{L}{L_0}\right) \quad (5)$$

The nominal stress is determined by Eq. (6), where F is the applied load and S_0 is the initial cross-sectional area. The true stress is given by Eq. (7) where F is the applied load and S is the cross-sectional area. S is estimated assuming that the total volume of the sample remained constant, according to Eq. (8). Both, stress at the yield point (σ_Y) and at break (σ_b) are determined.

$$\langle \sigma \rangle = \frac{F}{S_0} \quad (6)$$

$$\sigma = \frac{F}{S} \quad (7)$$

$$S = S_0 \times \frac{L_0}{L} \quad (8)$$

Young's modulus (E) is measured from the slope of the low strain region in the vicinity of 0 ($\sigma = \varepsilon = 0$).

3. Results and discussion

3.1. LCF analysis

Fig. 4 shows the size distributions of the different fractions (LCF_{0-1}, $LCF_{0-0.1}$, and $LCF_{0.1-1}$). LCF_{0-1} presents a double granulometric distribution, a population centred at 50 μm and another one at 700 μm. After sieving, we obtain two log-normal curves i.e., two homogeneous populations. A first distribution is centred at 50 μm and another one at 630 μm. Table 2 gives the different average sizes.

Figs. 5 and 6 show both fractions at different magnifications with various observation techniques, optical (Fig. 5) and electron (Fig. 6) microscopies. Fig. 5 (c and d) shows coloured fillers with acidified phloroglucinol which reveals phenolic compounds as the lignin. By contrast, we can see the cellulose organisation (microfibrils) in both samples. Optical micrographs (Fig. 5) show main differences between both fractions. $LCF_{0-0.1}$ looks like a powder with poorly-shaped fibres (Figs. 5a and c). $LCF_{0.1-1}$ is more fibrous; we show some pieces with the fibres network and the microfibrils (Figs. 5b and d). Observation carried out by SEM (see Fig. 6) shows very well the original organisation of the plant with the fibre organisation and the microfibrils. The fracture areas of the fibres networks and the subsequent defibrillations linked to the fillers preparation process are shown on $LCF_{0.1-1}$ SEM micrographs (see Figs. 6c and d). $LCF_{0-0.1}$ seems to be a mix of different shapes, fibrous (short and small pieces of fibres) and more or less spherical lignin-based particles. This diversity is due to the impact of the industrial fractionation process on the plant tissues. Wheat straw is composed of different tissues which are more or less destroyable during the process. On one hand, leaves, internodes and the parenchyma (see Fig. 7) are more particularly destroyable. On the other hand, the sclerenchyme and the fibres networks are more resistant.

Table 1 presents the chemical composition of different vegetable fibres. Compared to the others, wheat straw shows rather low cellulose content, a high lignin composition but also a high ash content linked to a high silica fraction. According to Zhang, Liu, and Li (1990), silica is mainly located on the leaves, 12% of ash in the leaves compared to e.g., 6% in the internodes. Average value is 7–8% of ash in the straw (Zhang et al., 1990).

Table 1 shows also the compositions of the different LCF fractions. We can show the effect of the wheat straw treatment. LCF shows higher lignin content. Assuming that the lignin which is insoluble is poorly affected by the hydrolysis process, the lignin quantity (in weight) stays constant from the initial wheat straw to the LCF_{0-1}. Then, lignin can be used as a reference. Cellulose and hemicellulose contents have been decreased under the hydrolysis treatment. Around 40% of the total cellulose and 85% of the hemicellulose have been eliminated during the process and collected mostly in the soluble fraction (see Table 1). We can notice that the process yield of hemicellulose sugars recovery is not total. By HPLC analysis, the hemicellulose composition can be given. Hemicellulose is composed with 96% of xylose, 3% of arabinose, and 1% of mannose.

On Table 1, $LCF_{0-0.1}$ shows intermediate values between $LCF_{0-0.1}$ and $LCF_{0.1-1}$. Comparing $LCF_{0-0.1}$ and $LCF_{0.1-1}$, we can notice that silica (ash) is more particularly present in the finest fraction. Then, $LCF_{0-0.1}$ must be composed, more particularly, of pieces of chopped leaves, which present higher silica content.

3.2. Biocomposites thermal properties

TGA has been carried out to evaluate the thermal behaviour of different biocomposites with filler content from 0 to 40 wt. Fig. 8 and Table 3 show the main results. Until more than 10 wt%, we cannot observe the transition linked to the fillers. At 300 °C, the variations of weight

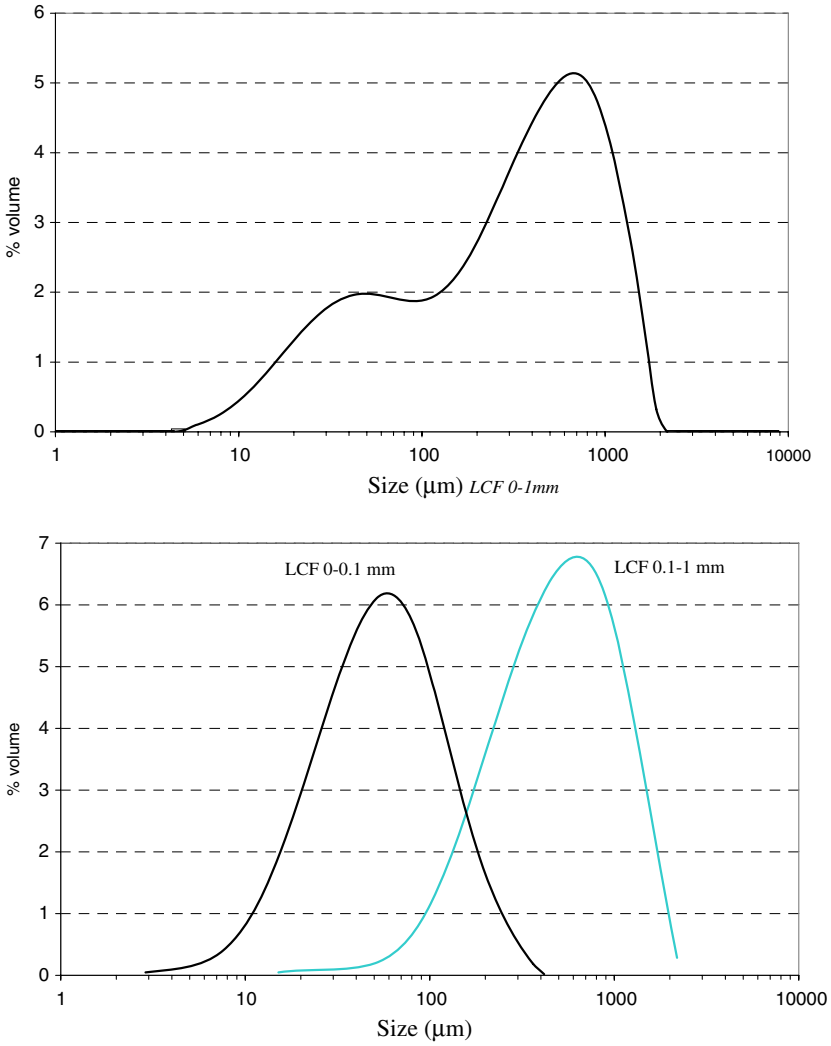

Fig. 4. Granulometric distributions of the different fillers ($LCF_{0–1}$, $LCF_{0–0.1}$, and $LCF_{0.1–1}$).

Table 2
Fillers average sizes

	$LCF_{0–1}$	$LCF_{0–0.1}$	$LCF_{0.1–1}$
Average size (microns) *Volume weighted*	320	50	460

losses are due the water uptake at equilibrium, which is higher for lignocellulosic fillers compared to PBAT. Then, the weight loss increases with filler content. This result can be obtained by the addition of the matrix water uptake (1%) and the filler water uptake (13–14%), corrected for the corresponding contents. Table 3 shows that the matrix degradation temperature and the corresponding onset increase with the filler content. These latter results are on agreement with Ruseckaite and Jiménez (2003) studies based on PCL matrix or with a previous work (Avérous & Boquillon, 2004) based on plasticized starch. In the same way, the filler degradation temperature (around 360 °C) is consistent with values obtained by other authors (Avérous & Boquillon, 2004; Ruseckaite & Jiménez, 2003) on lignocellulosic fillers. Additionally, we can show that LCF fillers are thermally stable up to 200 °C. The degradation behaviour of these fillers is then compatible with the plastic processing temperatures.

Fig. 9 shows the PBAT thermogram determined by DSC. Table 4 gives main thermal characteristics. Compared to most thermoplastics, T_g and T_f are rather low, and processing temperature is not high, around 130 °C. We can notice that this copolymer presents a single transition for T_g, T_c and T_m due to the repartition of the different sequences. These temperatures are intermediate between the data of both homopolymers, polybutylene adipate and polybutylene terephthalate (Chang & Tsai, 1994). At room temperature, PBAT is on the rubber plateau i.e., between T_g and T_f. Without knowing the theoretical enthalpy for 100% crystalline PBAT, we have used the approach presented by Herrera, Franco, Rodriguez-Galan, and Puiggali (2002). Theoretical enthalpy is calculated by the contribution of the different chain groups. The contributions of ester, methylene and p-phenylene groups are −2.5, 4.0, and 5.0 kJ/mol, respectively. The calculated value ($\Delta H_{100\%}$) is equal to 22.3 kJ/mol i.e., 114 J/g. The degree

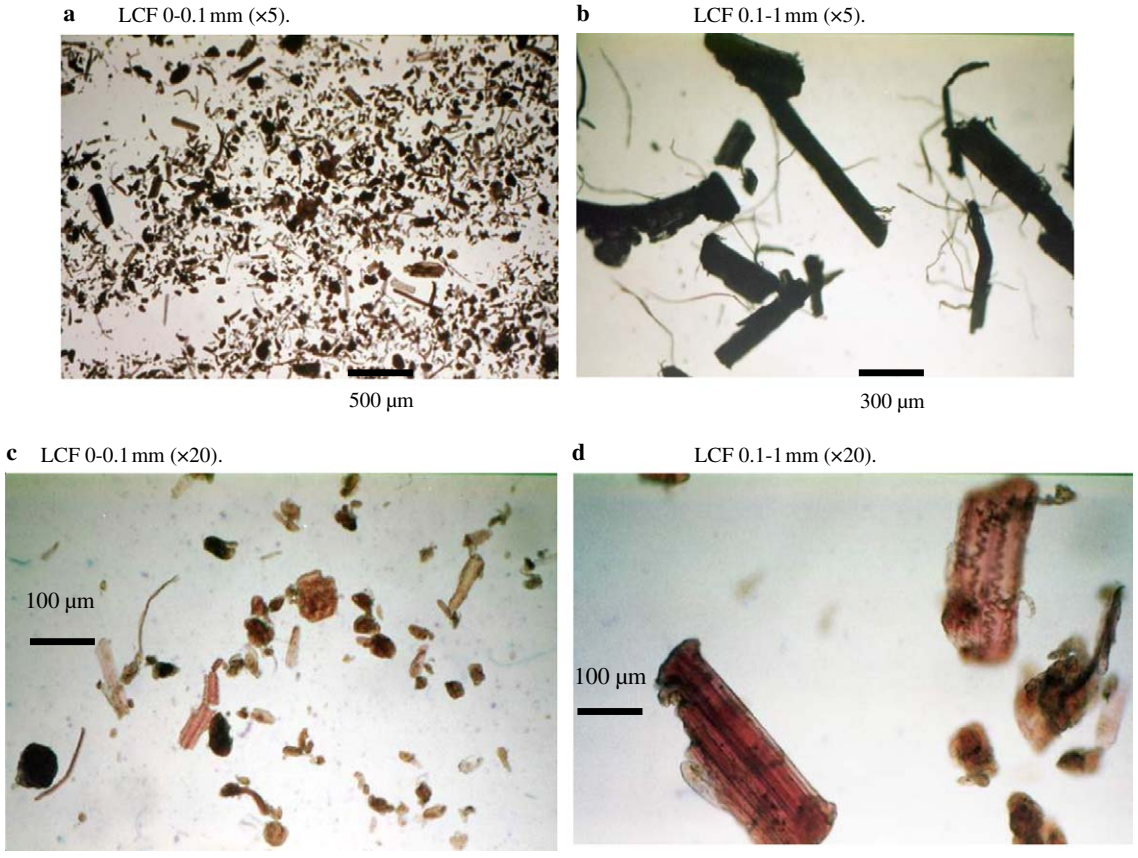

Fig. 5. Optical micrographs at different magnifications of $LCF_{0–0.1}$ (a and c) and $LCF_{0.1–1}$ (b and d). Samples c and d are treated with acidified phloroglucinol to reveal phenolic compounds.

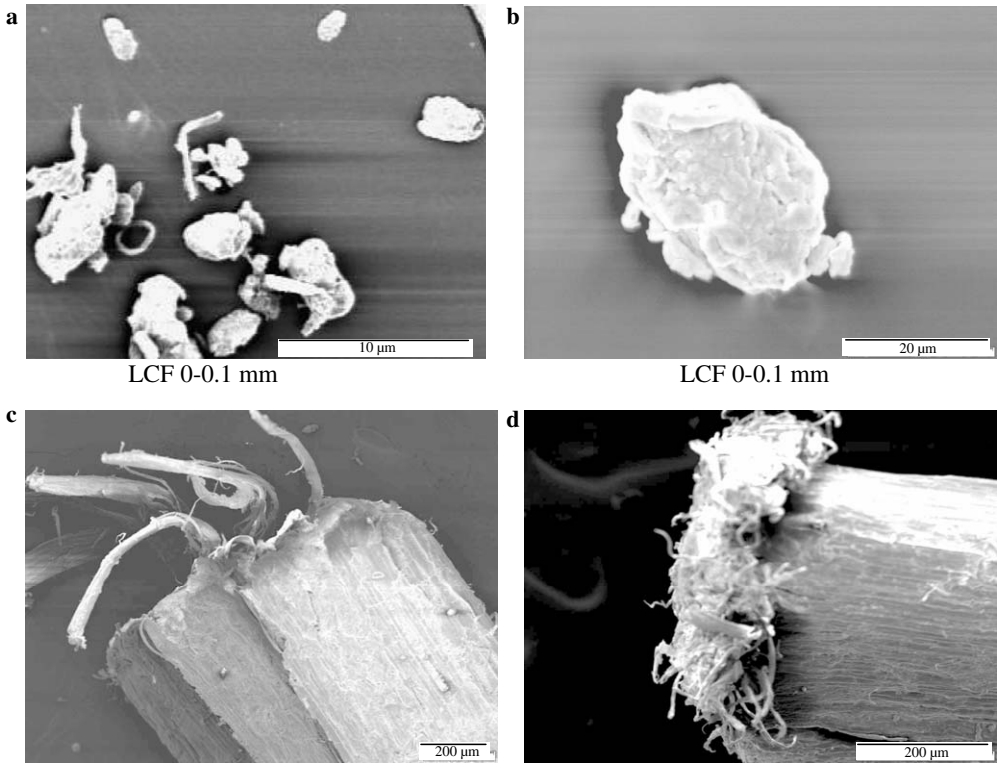

Fig. 6. Scanning electronic micrographs of $LCF_{0-0.1}$ (a and b) and $LCF_{0.1–1}$ (c and d).

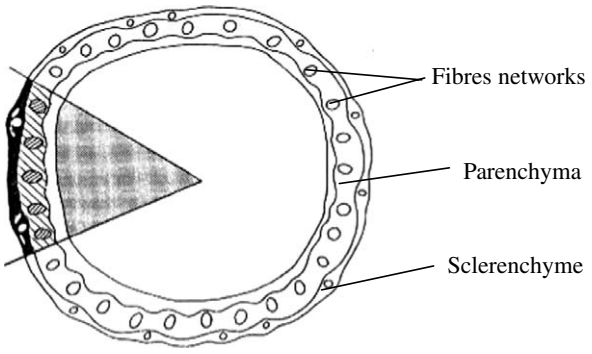

Fig. 7. Schema of the cross-section of a wheat straw stem with the different tissues.

of crystallinity (in %) is estimated with Eq. (3). PBAT crystallinity is rather low, around 12%. We can notice that the ΔCp gap at the glass transition is rather small. The different thermodynamic values are consistent with data obtained by other authors (Herrera et al., 2002).

Table 4 presents the different values obtained by DSC determinations on PBAT with increasing filler contents. As shown in Table 4, the addition of increasing amounts of LCF results in a slight but significant increase in T_g of PBAT, from −39.3 to −35.7 °C. According to Avella et al., this trend may be explained by intermolecular interactions between the hydroxyl groups of the fillers and the carbonyl groups of the PBAT ester functions. These hydrogen bonds would probably reduce the polymer mobility and then increase T_g values. The PBAT/LCF biocomposites do not show any significant variation of T_f, in agreement with the data of Avella et al. (2000). We have shown by SEC that the molecular weight variation is insignificant. We have not detected any chain degradation phenomena under the thermo-mechanical treatment. We can notice that crystallization and fusion heats decrease. This is due to a dilution effect linked to the fillers incorporation into the matrix. However, when the enthalpy is corrected by the filler content, these values stay rather constant e.g., $\Delta H_c'$ data (Table 4). The corrected heats of crystallization and fusion are equivalent; we do not have significant crystallization during the second scan. The heats of crystallization and fusion are equal to 13–14 J/g i.e., around 2.6 kJ/mol. The dilution effect seems also to affect ΔCp

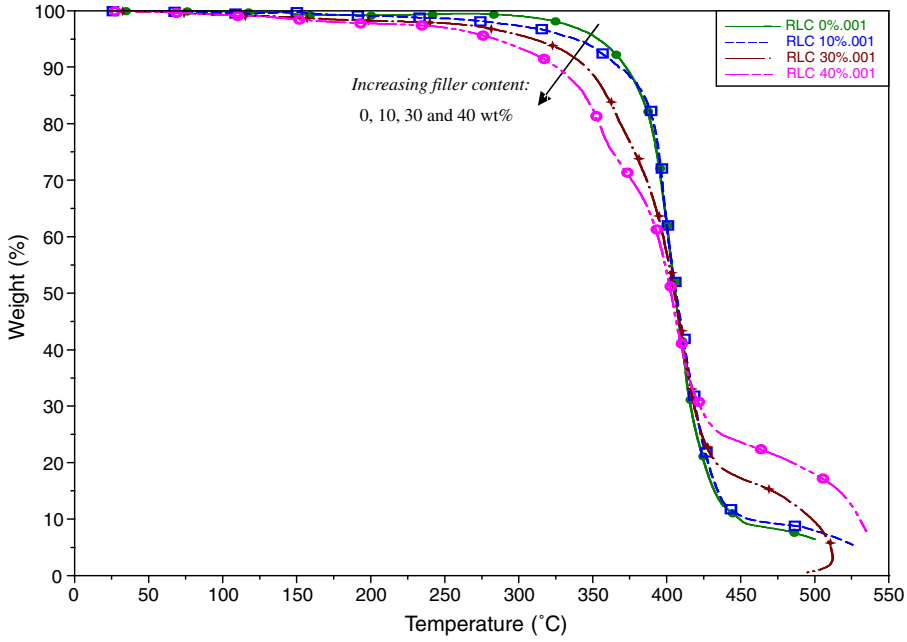

Fig. 8. TGA thermograms, mass fraction vs. temperature. TG of LCF-based biocomposites (0, 10, 30, and 40 wt % of LCF_{0-1}).

Table 3
Main TGA results

	Transition 1 –Filler–		Transition 2 –Matrix–		Loss of weight At 300 °C
	Onset 1	Degradation temperature maximum 1 of DTG	Onset 2	Degradation temperature maximum 2 of DTG	
PBAT	No visible "transition"		382 °C (15%)	410 °C (60%)	1%
LCF-10%			384 °C (15%)	411 °C (59%)	3%
LCF-30%	323 °C (6%)	364 °C (17%)	398 °C (61%)	413 °C (63%)	5%
LCF-40%	324 °C (10%)	357 °C (22%)	401 °C (48%)	421 °C (70%)	7%

Between brackets are given the total weight loss at the corresponding temperature.

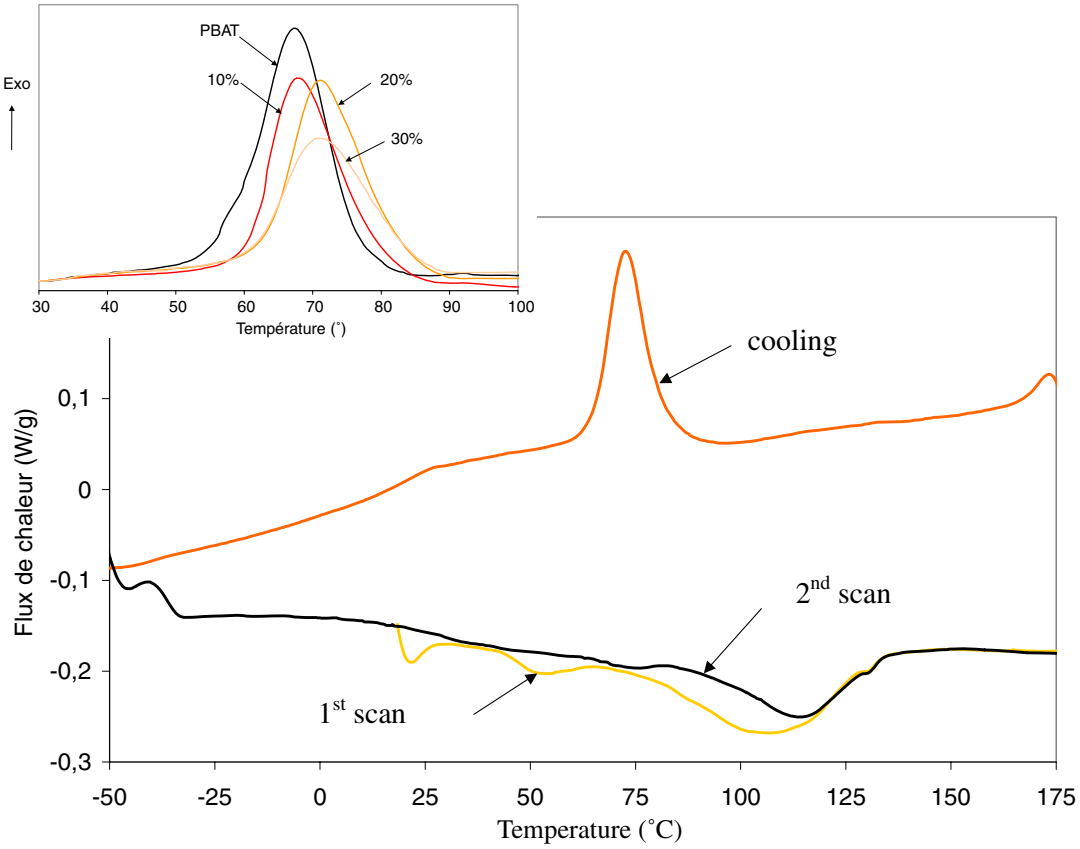

Fig. 9. DSC thermograms. Evolution of the heat flow vs. temperature for different biocomposites (0, 10, 20, 30 wt % of LCF_{0-1}).

Table 4
Main DSC results

Sample	T_g (°C)	ΔCp (W g^{-1})	T_c (°C)	T_i (°C)	ΔH_c (J g^{-1})	$\Delta H'_c$(J g^{-1})	T_f (°C)	ΔH_f (J g^{-1})	X_c (%)
PBAT	−39.3 ± 0.3	0.038 ± 0.001	68.0 ± 1.0	84 ± 1	13.5 ± 0.2	13.5 ± 0.2	113.9 ± 0.5	13.9 ± 0.3	12
PBAT-10%	−38.2 ± 0.2	0.028 ± 0.002	68.0 ± 0.4	87 ± 1	11.3 ± 0.1	12.6 ± 0.1	113.2 ± 0.7	11.7 ± 0.2	11
PBAT-20%	−36.6 ± 0.2	0.020 ± 0.001	71.0 ± 0.3	90 ± 1	11.4 ± 0.2	14.2 ± 0.3	113.8 ± 0.5	11.2 ± 0.4	12
PBAT-30%	−35.7 ± 0.2	0.010 ± 0.001	70.7 ± 0.3	91 ± 1	9.3 ± 0.5	13.3 ± 0.7	114.2 ± 0.6	10.0 ± 0.3	12

which tends to decrease with fillers incorporation. We can notice that an increase in LCF concentration does not affect the degree of PBAT crystallinity, which stays constant at around 12%. Fig. 9 shows crystallization curves of neat PBAT and PBAT/LCF biocomposites. The incorporation of LCF induces a slight but significant increase in T_c. This is probably linked to the reduction of the polymer mobility. The beginning of the crystallisation (T_i) during the cooling tends to increase with increasing fillers content. The fillers modify the crystallisation by increasing the number of nucleating sites. Fig. 9 shows that the PBAT crystallisation peak is Gaussian but with increasing fillers content, this peak becomes more and more asymmetric with an earlier crystallisation.

3.3. Biocomposite mechanical properties

Fig. 10 presents the mechanical behaviour (nominal values) under uniaxial tensile test of PBAT-based samples, with or without fillers. Stress–strain evolutions show that PBAT at room temperature is a ductile material with a high elongation at break (ε_b), more than 200%. This is consistent with T_g and T_f values. The matrix mechanical characteristics are given on Table 5. Fig. 10 shows also that even at high filler (LCF_{0-1}) content the material keeps its ductile character.

Concerning fillers, modulus evaluation is always problematic. The modulus has been evaluated following the approach developed by Gonzalez-Sanchez and Exposito-Alvarez (1999). Different PP composites had been processed with increasing LCF_{0-1} content (Le Digabel et al., 2004). The filler modulus has been estimated by fitting a semi-empirical Halpin–Tsai model on the evolution of the composites Young's modulus as a function of fillers volume fraction. By extrapolation at 100% of fillers (see Fig. 11), we obtain the filler modulus, estimated at 6.7 GPa. This value is consistent with wheat straw data given in the literature (Hornsby, Hinrichsen, & Tarverdi, 1997; Kronbergs, 2000) and with values obtained on different lignocellulosic materials (Young, 2004).

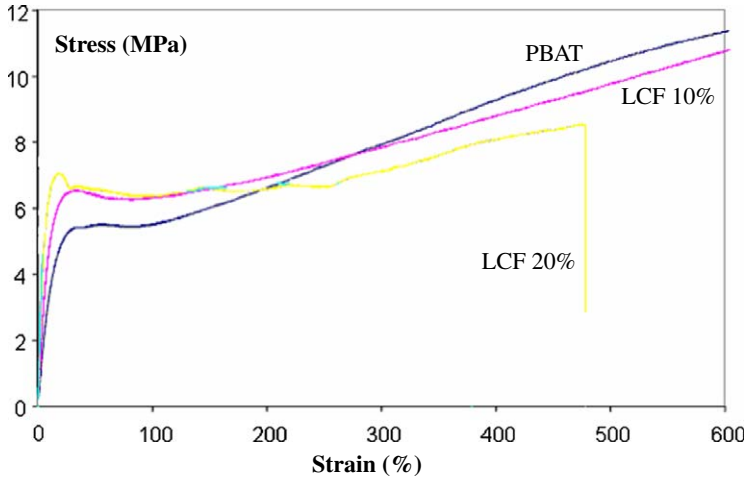

Fig. 10. Tensile mechanical behaviour (nominal values). Evolution of the stress vs. strain for different biocomposites (0, 10, 20 wt % of LCF_{0-1}).

Table 5
Tensile mechanical properties of PBAT

Modulus (MPa)	Yield stress (MPa)		Strength at break (MPa)		Elongation at the yield point (%)		Elongation at break (%)	
E	$\langle\sigma_Y\rangle$ Nominal	σ_Y True	$\langle\sigma_b\rangle$ Nominal	σ_b True	$\langle\varepsilon_Y\rangle$ Nominal	ε_Y True	$\langle\varepsilon_b\rangle$ Nominal	ε_b True
40	6	8	>12	>84	32	28	>600	>200

3.3.1. Effect of filler size

Fig. 12 shows, respectively, the variation of the modulus and the true values of ε_Y, ε_b, σ_Y, and σ_b for the different fillers fractions. These graphs present the mechanical behaviour of LCF_{0-1}, $LCF_{0-0.1}$, and $LCF_{0.1-1}$ based biocomposites reinforced at 30 wt%. These composites show a common behaviour compared to equivalent reinforced thermoplastics. LCF fractions act as reinforcing materials. By adding fillers, we obtain strong evolutions of the mechanical properties compared to the neat matrix; e.g. we increase the moduli of an order between 3.3 and 6.4 times. We can see that by increasing the filler size, we obtain both modulus and yield stress increases but also a decrease of ε_Y, ε_b, and σ_b. Concerning the modulus and the elongation at break, LCF_{0-1} shows intermediate values between $LCF_{0-0.1}$ and $LCF_{0.1-1}$ data. The smallest fraction ($LCF_{0-0.1}$) which is not the major fraction seems to drive LCF_{0-1} properties for the elongation at the yield point and the different tensile stresses. In any case, the biggest fraction ($LCF_{0.1-1}$) fully drives the LCF_{0-1} tensile properties

3.3.2. Effect of the filler content

To estimate the effect of the filler, composite/matrix ratios are calculated from tensile test results. In Fig. 13 are shown different variations of mechanical parameters versus the fillers (LCF_{0-1}) volume fraction. Volume fractions (ϕ) are determined from the fractions in weight

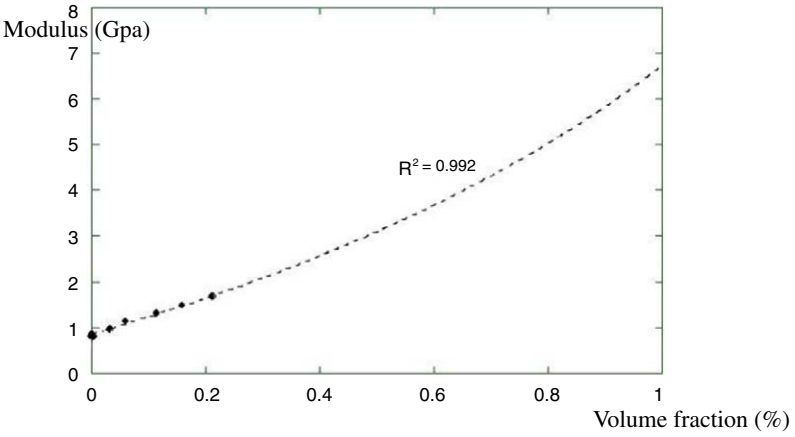

Fig. 11. Halpin-Tsai fitting on the evolution of the modulus of LCF_{0-1}-based PP composites vs. filler volume fraction.

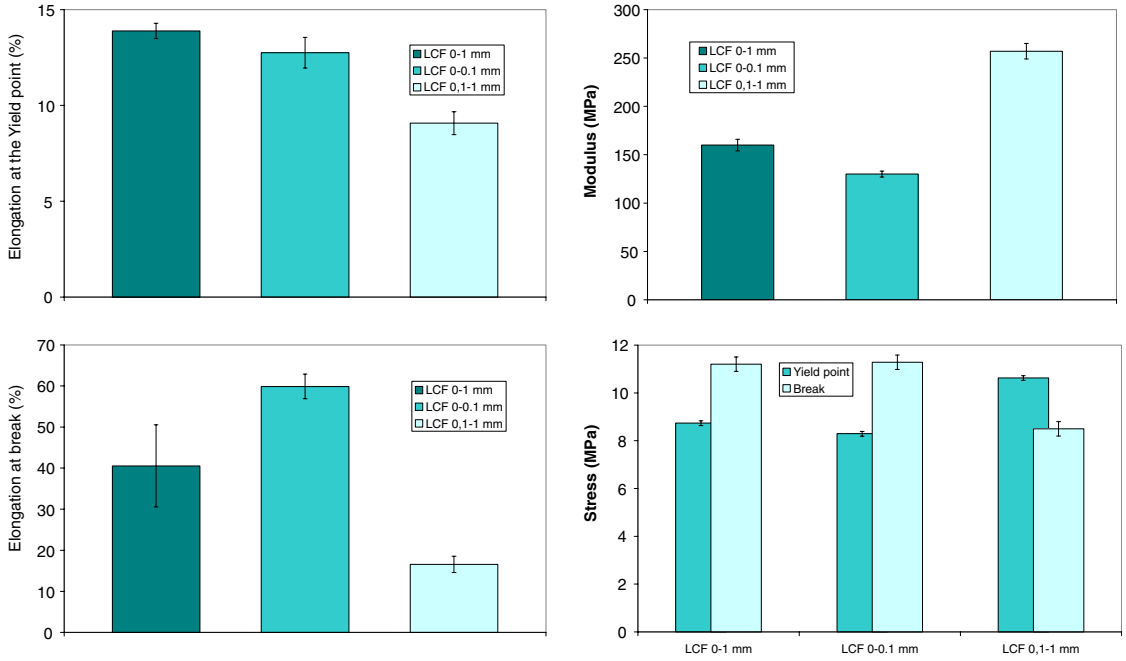

Fig. 12. Tensile mechanical properties- Impact of the filler fraction ($LCF_{0–1}$, $LCF_{0–0.1}$, and $LCF_{0.1–1}$) at 30 wt %.

(ww) according to Eq. (9), using the density of each component (d). LCF density is 1.45 g/cm^3. This value has been determined by pycnometry measurements on 10, 20, and 30 wt% $LCF_{0–1}$ biocomposites. This data is on agreement with cellulose and lignin densities.

$$\phi_i = \frac{ww_i/d_i}{\sum_i ww_i/d_i} \tag{9}$$

Determining composites/matrix ratios, Fig. 14 shows that yield stress ratios are adjusted on a positive linear trend (slope = 0.057) according the filler volume fraction. The yield strain ratios are fitted on a negative exponential curve (coefficient = −0.072).

3.3.3. Percolation effect and moduli modelling

We can notice on Fig. 14 that, by increasing the volume fraction, we obtain a modulus evolution with an increase of the slope. According to the literature, the percolation threshold obtained by 2D/3D simulations (Favier, Dendievel, Canova, Cavaille, & Gilormini, 1997) for such filler length is around 10 wt%. But the influence on the modulus of this percolation threshold is too low to be taken into account on a model contrary to e.g., nanocomposite systems (Favier et al., 1997), where the impact of the threshold on the modulus is higher.

To fit and to estimate the modulus evolution, different simple models have been tested such as the models of Voigt (Eq. (10)), Reuss (Eq. (11)), and Takayanagi (Eq. (12)). The composite modulus (E_c) is determined from E_f and E_m, which are the filler and the matrix moduli, respectively.

The lowest and the highest moduli estimations are given by the serial model from Reuss ($E_{c(R)}$) and by the parallel model from Voigt ($E_{c(V)}$), respectively. The modulus value should be comprised between these two boundaries.

$$E_{c(V)} = \phi_m E_m + \phi_f E_f \tag{10}$$

$$\frac{1}{E_{c(R)}} = \frac{\phi_m}{E_m} + \frac{\phi_f}{E_f} \tag{11}$$

Takayanagi's model is a phenomenological model obtained by combination of serial and parallel models. The composite modulus ($E_{c(T)}$) is determined by the Eq. (12) with λ, an adjustment parameter (Nielsen & Landel, 1994).

$$E_{c(T)} = (1-\lambda)E_m + \frac{\lambda}{\frac{1-\phi_f}{E_m} + \frac{\phi_f}{E_f}} \tag{12}$$

Fig. 15 shows that Takayanagi's equation seems to be an excellent model to predict the modulus evolution in the range 0–30 wt% of filler. The parameter (λ) has been determined by adjustment at 4.5. Reuss and Voigt's models are not well adapted to estimate correctly the composite moduli. This is because the matrix and the fillers mechanical characteristics are too different. But, we can show that the composite moduli are comprised between both boundaries, $E_{c(R)}$ and $E_{c(V)}$.

4. Conclusion

Different biocomposites have been produced by introduction of lignocellulosic fillers into aromatic biodegradable polyester, polybutylene adipate-co-terephthalate. The paper is targeted toward presentation of the different processes and their corresponding product characteristics (from the compounds to the composites). The matrix has been carefully analysed e.g., we have determined by

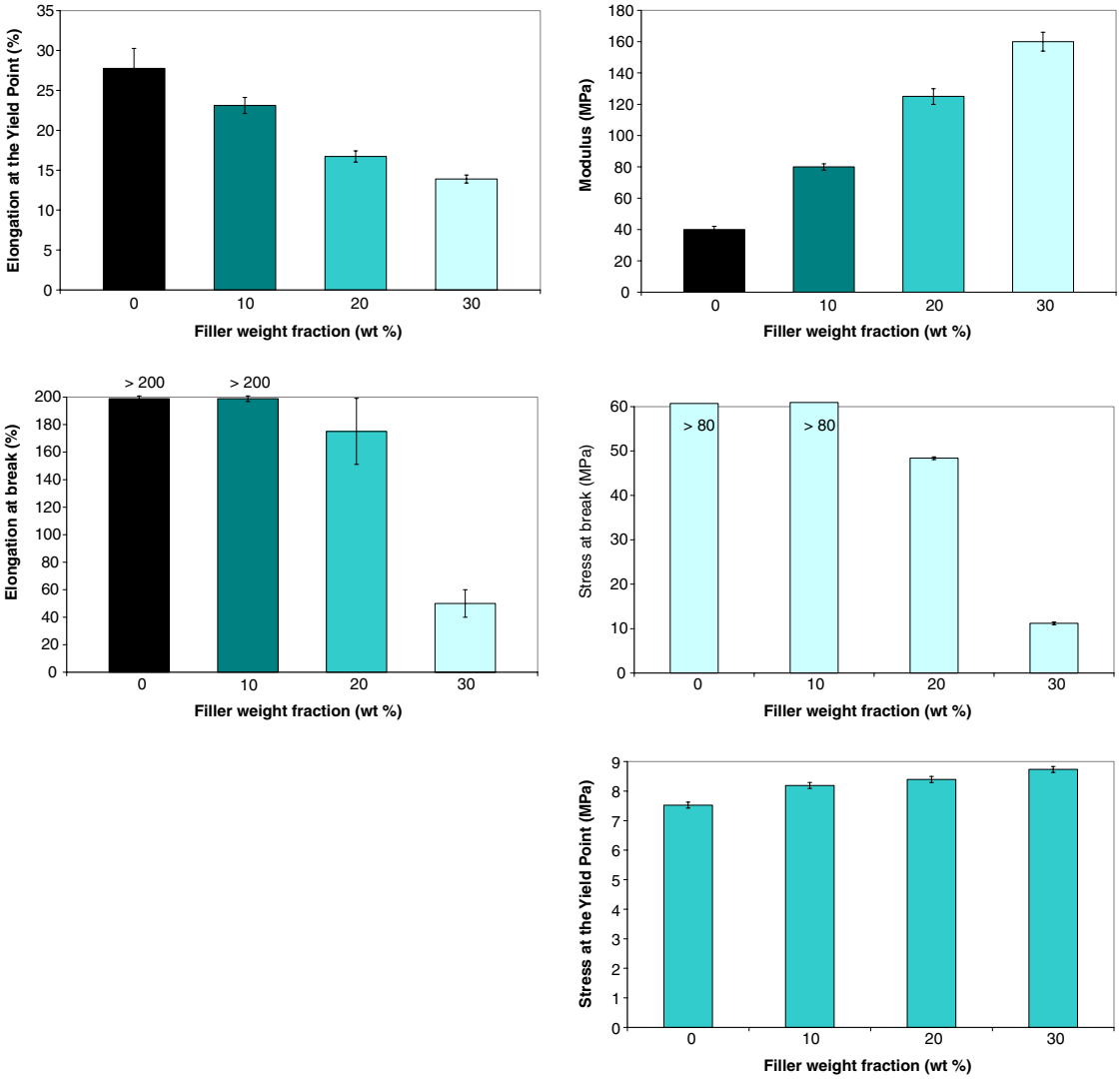

Fig. 13. Tensile mechanical properties – Impact of the filler (LCF_{0-1}) content (from 0 to 30 wt%).

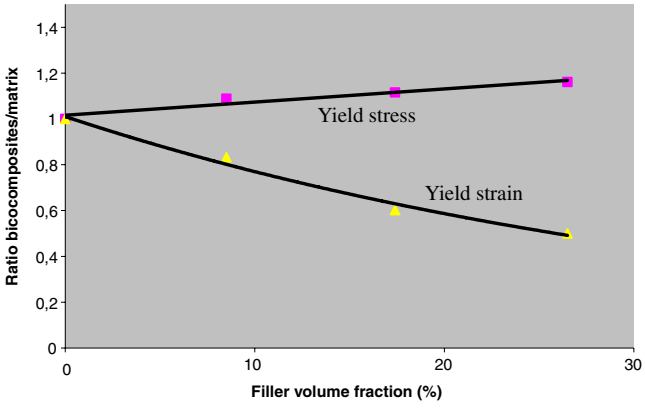

Fig. 14. Fittings on the evolution of some tensile mechanical properties (Yield stress and strain) vs. volume filler (LCF_{0-1}) content.

NMR the ratio between the co-monomers and by SEC, the molecular weights. The fillers have been obtained from wheat straw after an acid hydrolysis step to eliminate main hemicellulose and after a fragmentation phase. The dried fillers have been sieved. We have obtained a population with a heterogeneous size distribution. After a second sieving, we have achieved two homogeneous fractions with two average sizes, 45 and 460 microns. The three types of fillers have been carefully characterised. These fillers present high lignin contents. We have analysed the impact of the introduction of these fillers into the matrix through thermal and mechanical analysis. By TGA, we have shown that the fillers degradation temperature is higher enough to be compatible with the processing temperatures (extrusion and injection moulding). Additionally, adding filler has increased the thermal degradation temperature of the matrix, as a function of the reinforcing content. By DSC, we have shown that the filler did not modify the level of crystallinity of the matrix, but the fillers have induced a nucleating effect. We have obtained a T_g increase linked to a reduction of the chain mobility. This increase has been associated with an increase of the T_c and T_f. We have determined the heat of fusion at 12–13 J/g. The impact of the fillers size and content have been analysed through uniaxial

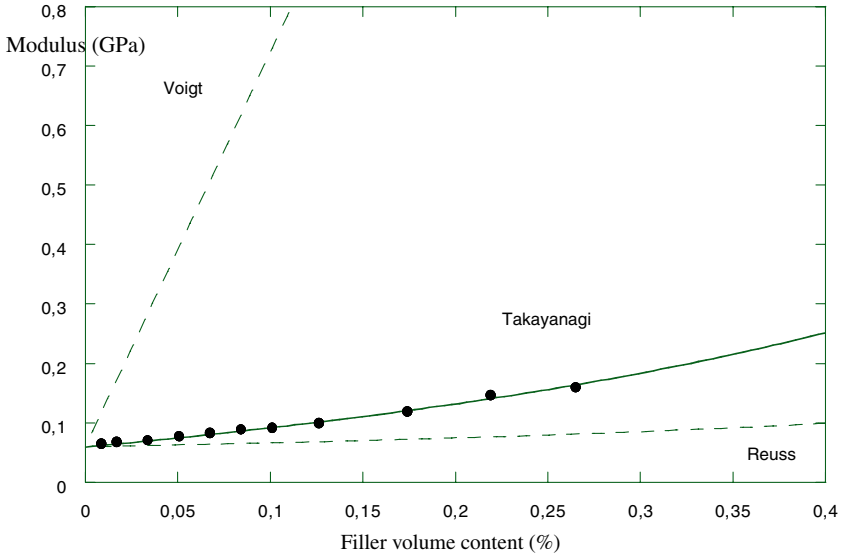

Fig. 15. Fittings on the evolution of the modulus of LCF_{0-1}-based biocomposites vs. filler volume fraction content (Takayanagi, Voigt, and Reuss models).

tensile test results. Compared to common reinforced thermoplastics, these biocomposites have shown a similar behaviour. The evolution of the composite mechanical behaviour was due to a reinforcing effect associated to quite good fillers-matrix interactions. To predict the modulus evolution, we have shown that Takayanagi's equation is an accurate and a simple answer to evaluate the modulus in a range comprises between 0 and 30 wt%.

The association of biodegradable polymer with these lignocellulosic fillers is a good solution to overcome primary issues with biodegradable polymers, i.e., the cost and the mechanical properties. Then, the different associations we can obtain can fulfill the requirements of different fields of application, such as non-food packaging or other short-lived applications (agriculture, sport, etc.) where long-lasting polymers are not entirely adequate. In addition, these materials are in agreement with the emergent concept of sustainable development.

Acknowledgements

This work is funded by Europol'Agro through a research program devoted to materials based on agricultural resources. The authors thank Zuzana Kadlecova (VSCHT-Czech Rep./ECPM-France) and Cheng Ngov (ECPM-France) for NMR and SEC determinations, respectively. Besides, we thank Pr. Monties for his great investment in this project.

References

Avella, M., La Rota, G., Martuscelli, E., Raimo, M., Sadocco, P., Elegir, G., & Riva, R. (2000). Poly(3-hydroxybutyrate-co-3-hydroxyvalerate) and wheat straw fibre composites: thermal, mechanical properties and biodegradation behaviour. *Journal of Materials Science, 35*(4), 829–836.

Avérous, L. (2004). Biodegradable multiphase systems based on plasticized starch: a review. *Journal of Macromolecular Science – Part C Polymer Reviews, C4*(3), 231–274.

Avérous, L., & Boquillon, N. (2004). Biocomposites based on plasticized starch: thermal and mechanical behaviours. *Carbohydrate Polymers, 56*(2), 111–122.

Avérous, L., Fringant, C., & Moro, L. (2001). Plasticized starch-cellulose interactions in polysaccharide composites. *Polymer, 42*(15), 6571–6578.

Bledzki, A. K., & Gassan, J. (1999). Composites reinforced with cellulose-based fibres. *Progress in Polymer Science, 24*, 221–274.

Bourban, Ch., Karamuk, E., De Fondaumiere, M. J., Ruffieux, K., Mayer, J., & Wintermantel, E. (1997). Processing and characterization of a new biodegradable composite made of a PHB/V matrix and regenerated cellulosic fibers. *Journal of Environmental Polymer Degradation, 5*(3), 159–166.

Chang, S.-J., & Tsai, H. B. (1994). Copolyesters. VII. Thermal transitions of poly(butylene terephtalate-co-adipate)s. *Journal of Applied Polymer Science, 51*, 999–1004.

Dufresne, A., Dupeyre, D., & Paillet, M. (2003). Lignocellulosic flour-reinforced poly(hydroxybutyrate-co-valerate) composites. *Journal of Applied Polymer Science, 87*(8), 1302–1315.

Favier, V., Dendievel, R., Canova, G., Cavaille, J. Y., & Gilormini, P. (1997). Simulation and modeling of three-dimensional percolating structures: case of a latex matrix reinforced by a network of cellulose fibers. *Acta Materialia, 45*(4), 1557–1565.

Fernandes, E. G., Pietrini, M., & Chiellini, E. (2004). Bio-based polymeric composites comprising wood flour as filler. *Biomacromolecules, 5*(4), 1200–1205.

Gonzalez-Sanchez, C., & Exposito-Alvarez, L. A. (1999). Micromechanics of lignin/polypropylene composites suitable for industrial applications. *Angewandte Makromolekulare Chemie, 272*, 65–70.

Herrera, R., Franco, L., Rodriguez-Galan, A., & Puiggali, J. (2002). Characterization and degradation behavior of poly(butylene adipate-co-terephthalate)s. *Journal of Polymer Science: Part A: Polymer Chemistry, 40*, 4141–4157.

Hornsby, P. R., Hinrichsen, E., & Tarverdi, K. (1997). Preparation and properties of polypropylene composites reinforced with wheat and flax straw fibers. Part II: Analysis of composite microstructure and mechanical properties. *Journal of Materials Science, 32*, 1009–1015.

Kitagawa, K., Watanabe, D., Mizoguchi, M., & Hamada, H. (2002). Bamboo particle filled composites. *Polymer Processing Symposium PPS-18*, (Guimares) Portugal.

Kronbergs, E. (2000). Mechanical strength testing of stalk materials and compacting energy evaluation. *Industrial Crops and Products, 11*, 211–216.

Le Digabel, F., Boquillon, N., Dole, P., Monties, B., & Avérous, L. (2004). Properties of thermoplastic composites based on wheat straw lignocellulosic fillers. *Journal of Applied Polymer Science, 93*(1), 428–436.

Le Digabel, F. (2004). Incorporation de co-produits de paille de blé dans des matrices thermoplastiques. Approche de la compatibilité charge-matrice et propriétés des composites. Ph.D. Thesis URCA Reims (France) 198p.

Lequart, C., Ruel, K., Lapierre, C., Pollet, B., & Kurek, B. (2000). Abiotic and enzymatic degradation of wheat straw cell wall: a biochemical and ultrastructural investigation. *Journal of Biotechnology, 80*, 249–259.

Levit, M. R., Farrel, R. E., Gross, R. A., & McCarthy, S. P. (1996). Composites based on poly(lactic acid) and cellulosic materials: mechanical properties and biodegradability. *Annual Technical Conference – Society of Plastics Engineers 54th*, Vol. 2, pp. 1387–1391.

Luo, S., & Netravali, A. N. (1999). Interfacial and mechanical properties of environment-friendly "green" composites made from pineapple fibers and poly(hydroxybutyrate-co-valerate) resin. *Journal of Materials Science, 34*(15), 3709–3719.

Mohanty, A. K., Khan, M. A., & Hinrichsen, G. (2000a). Surface modification of jute and its influence on performance of biodegradable jute-fabric/Biopol composites. *Composites Science and Technology, 60*(7), 1115–1124.

Mohanty, A. K., Khan, M. A., & Hinrichsen, G. (2000b). Influence of chemical surface modification on the properties of biodegradable jute fabrics – polyester amide composites. *Composites Part A: Applied Science and Manufacturing, 31*(2), 143–150.

Mohanty, A. K., Misra, M., & Hinrichsen, G. (2000). Biofibres, biodegradable polymer and composites: an overview. *Macromolecular Materials and Engineering*(276/277), 1–24.

Monties, B. (1984). Dosage de la lignine insoluble en milieu acide. *Agronomie, 4*, 387–392.

Netravali, A. N., & Chabba, S. (2003). Composites get greener. *Materials Today, 6*(4), 22–29.

Nielsen, L. E., & Landel, R. F. (1994). *Mechanical properties of polymers and Composites*. New York: Marcel Dekker.

Nishino, T., Hirao, K., Kotera, M., Nakamae, K., & Inagaki, H. (2003). Kenaf reinforced biodegradable composite. *Composites Science and Technology, 63*(9), 1281–1286.

Oksman, K., Skrifvars, M., & Selin, J.-F. (2003). Natural fibres as reinforcement in polylactic acid (PLA) composites. *Composites Science and Technology, 63*(9), 1317–1324.

Plackett, D., Logstrup Andersen, T., Batsberg Pedersen, W., & Nielsen, L. (2003). Biodegradable composites based on l-polylactide and jute fibres. *Composites Science and Technology, 63*(9), 1287–1296.

Roller, M. (1990). Valorisation non alimentaire des co-produits du blé: contribution à l'extraction et à la purification d'hexoses et de pentoses en vue de la synthèse de polyglycosides d'alkyles. *Ph.D. Thesis, Institut National Agronomique Paris Grignon* (France), 214p.

Ruseckaite, C. R., & Jiménez, A. (2003). Thermal degradation of mixtures of polycaprolactone with cellulose derivatives. *Polymer Degradation and Stability, 81*(2), 353–358.

Saheb, D. N., & Jog, J. P. (1999). Natural fiber polymer composites: a review. *Advances in Polymer Technology, 18*(4), 351–363.

Shibata, M., Takachiyo, K., Ozawa, K., Yosomiya, R., & Takeishi, H. (2002). Biodegradable polyester composites reinforced with short abaca fiber. *Journal of Applied Polymer Science, 85*(1), 129–138.

Van de Velde, K., & Kiekens, P. (2002). Biopolymers: overview of several properties and consequences on their applications. *Polymer Testing, 21*(4), 433–442.

Wollerdorfer, M., & Bader, H. (1998). Influence of natural fibres on the mechanical properties of biodegradable polymers. *Industrial Crops and Products, 8*, 105–112.

Young, R. A. (2004). Vegetable Fibers. In H. F. Mark (Ed.) (third ed.). *Encyclopedia of Polymer Science and Technology, Part 3* (Vol. 12). NY: Wiley.

Zhang, D. X., Liu, & Li, Z. (1990). The analyses of fiber morphology and chemical composition of the differents of wheat straw, *China Pulp and Paper*, pp. 16–21.